Supplementary Materials

Deep-Learning Enabled Rapid and Low-Cost Detection of Microplastics in Consumer Products Following On-site Extraction and Image Processing

Md. Zayed Bin Zahir Arju,[†] Nafisa Amin Hridi,[†] Lamiya Dewan,[†] Suhaila,[‡] Md. Nurul Amin ,[¶] Taslim Ur Rashid,[¶] Abul Kalam Azad,[†] Sejuti Rahman,[§] Mainul Hossain,[*,†] and Ahsan Habib[*,†]

†*Department of Electrical and Electronic Engineering, University of Dhaka, Dhaka-1000, Bangladesh*

‡*Department of Computer Science and Engineering, Independent University, Bangladesh, Dhaka-1229, Bangladesh*

¶*Department of Applied Chemistry and Chemical Engineering, University of Dhaka, Dhaka-1000, Bangladesh*

§*Department of Robotics and Mechatronics Engineering, University of Dhaka, Dhaka-1000, Bangladesh*

E-mail: mainul.eee@du.ac.bd; mahabib@du.ac.bd

Supplementary Text 1: Preparation of Image Dataset

We used a "TinyScope" microscope attachment to capture images of the plastics. The raw images were then processed using ImageJ software. First, we resized each image to 888×960 pixels (Image > Adjust > Canvas Size). Next, we applied a bandpass filter (Process > FFT > Bandpass Filter) with the parameters 'Filter large structures' set to 40 pixels and 'Filter small structures' set to 3 pixels. We then converted the images to 8-bit (Image > Type > 8-bit) and fine-tuned the threshold values to generate the desired mask image (Image > Adjust > Threshold). Keeping dark background mode and B&W mode selected, we set lower threshold level at 126 and higher threshold level at 255. The resulting masked or thresholded images, shown in Fig. S2, have a white background with darkened areas identified as microplastic elements.[1]

Following the preprocessing steps where images were masked or thresholded, we utilized the annotation software "Label Studio"[2] to manually label the target objects. Each object of interest was annotated as a single class, designated "Microplastic". In this process, the darkened regions of the images were labeled as Microplastic, while the remaining white portions were treated as background. After completing the annotation across the entire dataset, the image files and corresponding label files were organized according to the YOLOv5 format to ensure compatibility for model train processing. The model was subsequently trained and evaluated based on key performance evaluation metrics, including mean Average Precision (mAP@50), Precision, Recall, Box Loss, and Object Loss. A comprehensive overview of the workflow is illustrated in Fig. S3.

Supplementary Text 2: COD Analysis

Analytical-grade reagents were used throughout the experiment. Distilled water was used wherever dilution was required. A series of similar 10 mL microplastic extraction solutions were prepared from teabag samples. After the addition of $ZnCl_2$ and H_2O_2 solutions, the solutions were put through the vortex mixer. A subset of the prepared samples was subjected

to five minutes of agitation at three different frequencies: 5 Hz (300 rpm), 20 Hz (1200 rpm), and 50 Hz (3000 rpm), while the remaining samples were left unagitated at 0 Hz. All the samples were transferred into 250 mL conical flasks. 90 mL distilled water was added to make a total solution of 100 mL. 10 mL of diluted H_2SO_4 solution and 10 mL of 0.02 M $KMnO_4$ digestion solution were added carefully to each of them. The samples were placed in a water bath and heated for 30 minutes at 94°–98° C. After that, 10 mL of 0.05 M $(NH_4)_2C_2O_4$ solution was added to the warm solution and shaken manually until completely transparent. By using titration, the amount of $KMnO_4$ required to oxidize the remaining $(NH_4)_2C_2O_4$ in the solution was determined.[3,4] This amount is equivalent to the $KMnO_4$ required to oxidize the residual organic and inorganic materials present in the sample solutions. The suggested $KMnO_4$ techniques were used to determine the COD values of the microplastic solutions that were agitated at different frequencies. The results are presented in table and graph at Fig. 2 in the main manuscript. The COD was calculated using the following formula:

$$\text{COD} = \frac{0.8 \times V' \times 1000}{V} \text{ mgL}^{-1}\ O_2$$

Where, V': The average volume of 0.02 M $KMnO_4$ solution used to titrate the sample, mL.
V: Volume of water sample used for the determination, mL.
The sample solutions, upon adding the reagents, undergo the following reaction:

$$5(NH_4)_2C_2O_4(aq) + 2KMnO_4(aq) + 8H_2SO_4(aq) \rightarrow 2MnSO_4(aq) + 10CO_2(g) + K_2SO_4(aq) + 5(NH_4)_2SO_4(aq) + 8H_2O(aq)$$

This is a redox reaction, which turns the deep purple tone of $KMnO_4$ completely transparent. However, due to the presence of organic and inorganic matter in the samples, a fraction of $KMnO_4$ digests those organics, which reduces the overall amount of $KMnO_4$ in the solution. Thus, $KMnO_4$ acts as the limiting reagent upon the addition of $(NH_4)_2C_2O_4$ in the solution.

We used titration with $KMnO_4$ in order to obtain the additional amount required to oxidize the $(NH_4)_2C_2O_4$ present in the sample. The moment the solution gets back a light purple stain from the $KMnO_4$, the amount was noted. The required amount came out to be 5.1 mL for the unagitated (0 Hz) sample, 5.0 mL for the 5 Hz sample, 4.5 mL for the 20 Hz sample, and 4.1 mL for the 50 Hz sample. The experiment was repeated three times, and similar trends were observed throughout.

Supplementary Figure S1: Schematic representation of the workflow

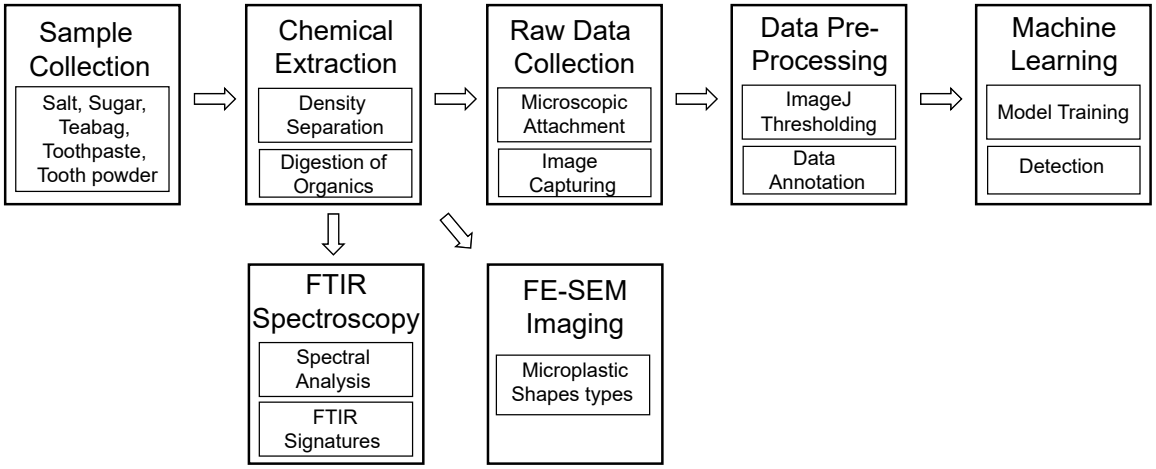

Figure S1: Schematic representation of the microplastic extraction, analysis, and detection workflow. The process includes sample collection (salt, sugar, teabag, toothpaste, and tooth powder), chemical extraction (density separation and digestion of organics), and raw data collection using a microscopic attachment for imaging. The captured images undergo pre-processing (thresholding and annotation) before being used for machine learning-based model training and detection. Additionally, FTIR spectroscopy is performed for spectral analysis, and FE-SEM imaging is used to examine microplastic shapes.

Supplementary Figure S2: Image thresholding

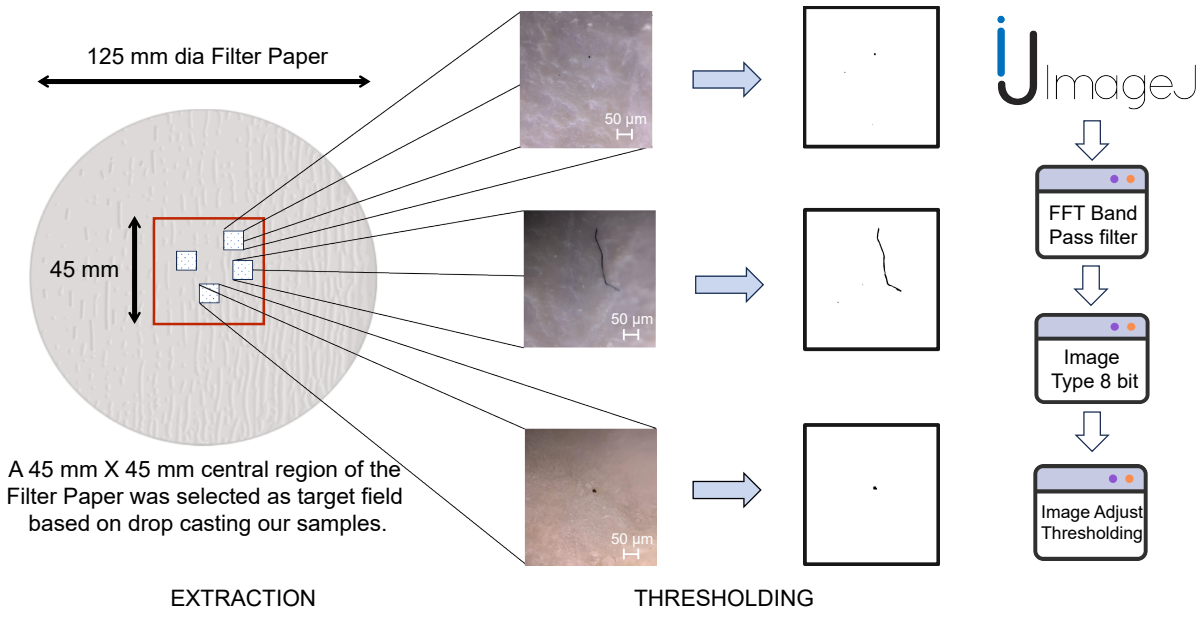

Figure S2: The photographs were captured from the primary region of focus, specifically the central portion of the filter paper measuring $45mm \times 45mm$. Subsequently, these unprocessed raw photographs underwent ImageJ binary thresholding and fine-tuning adjustments. The resulting images demonstrate tiny plastic particles against a white background, acquired through ImageJ examination and combined imaging methods.

Supplementary Figure S3: Image data processing and training

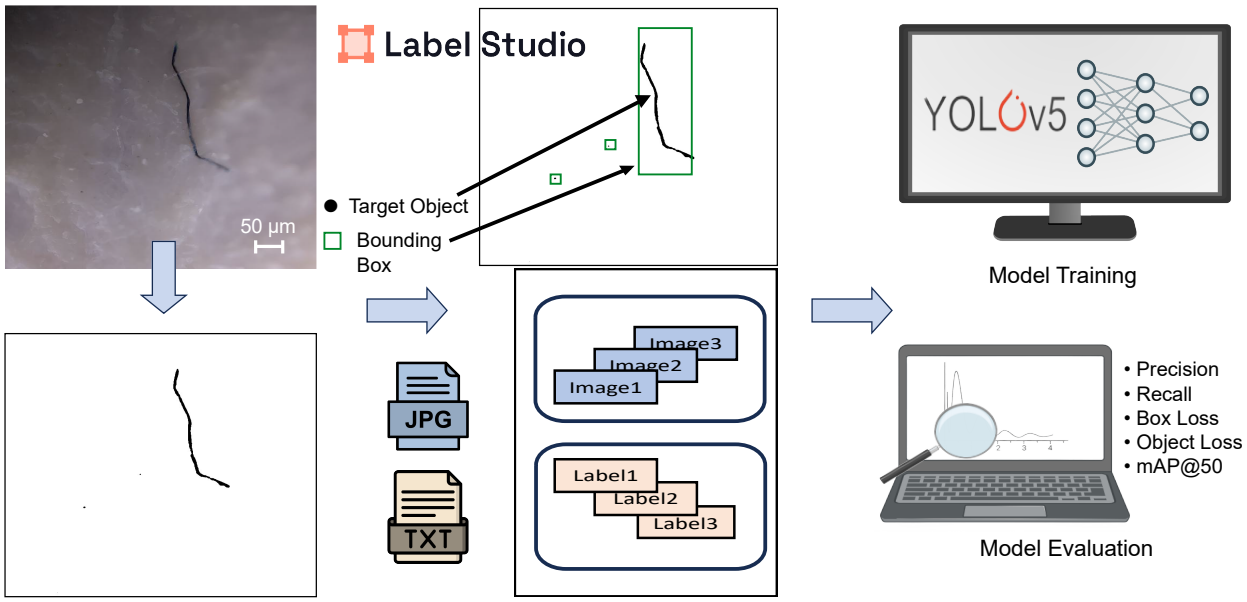

Figure S3: (a) The process involves annotating masked or thresholded images using the "Label Studio" labeling software. Target elements are demarcated by black objects enclosed within green squares, while the background is illustrated in white. (b) Subsequently, the annotated data is extracted from the software in .jpg and .txt formats, which are then randomly partitioned into training, validation, and test datasets. (c) Finally, the preprocessed dataset is utilized as input for the YOLOv5 model, followed by an evaluation based on mentioned performance metrics.

Supplementary Figure S4: FE-SEM images of remaining two categories.

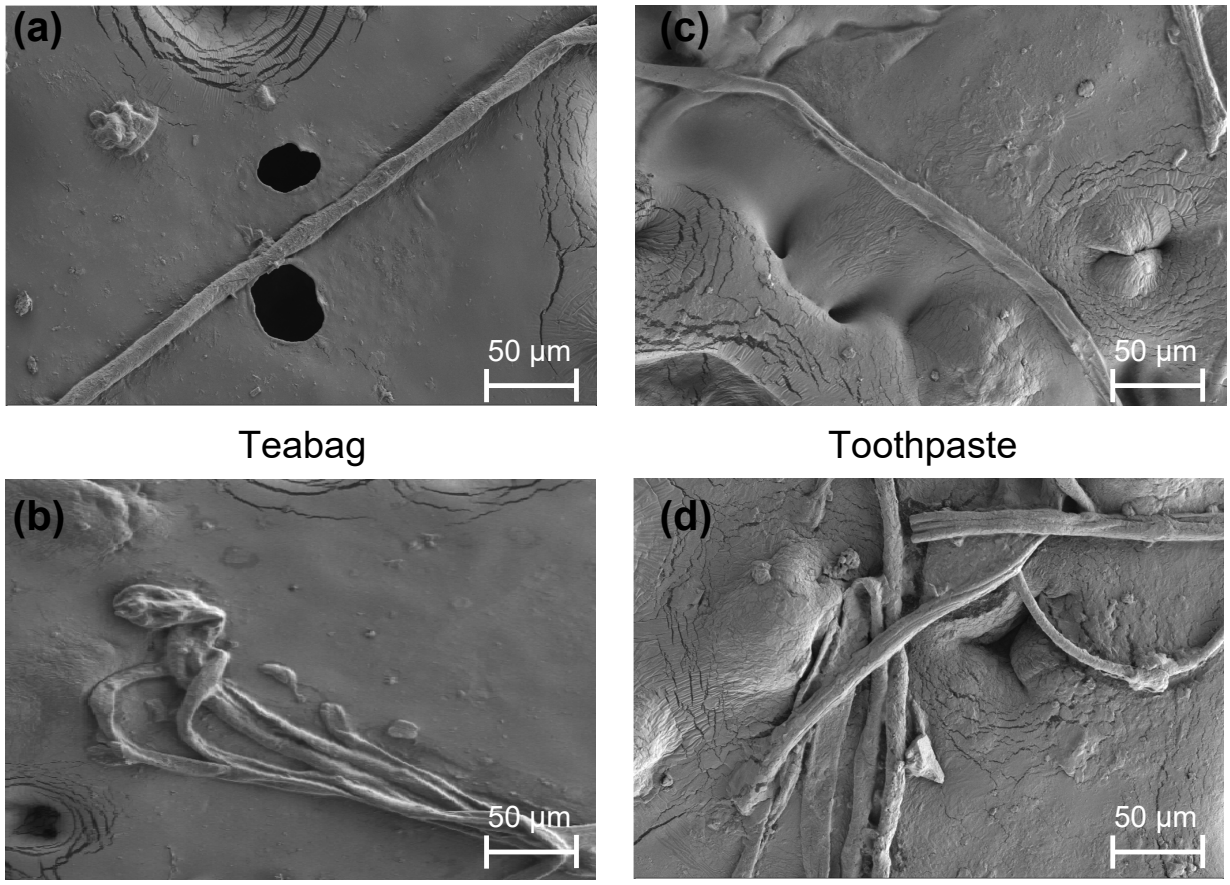

Figure S4: Field-emission scanning electron microscopy (FE-SEM) images of the extracted samples from Teabag and Toothpaste. The images reveal detailed morphological characteristics of the microplastics. The samples are mainly fiber-type microplastics, as shown in images (a), (b), (c), and (d), and fragment-type microplastics, as seen in images (b) and (d). The scale bar in each image represents 50 µm.

Supplementary Figure S5: Model Evaluation with Object Loss and mAP@50

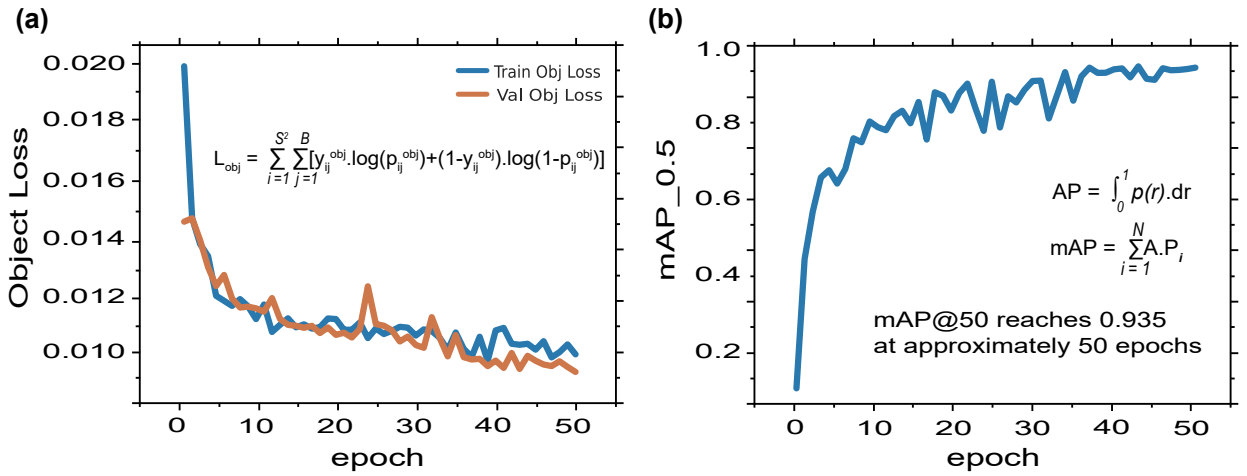

Figure S5: Evaluation of the YOLOv5 model trained for object detection. (a) The object loss for both training (blue) and validation (orange) decreases over 50 epochs, suggesting that the model is improving in accurately detecting whether objects are present in the images as training advances. The objectness loss L_{obj} improves the model's ability to detect objects by penalizing incorrect predictions. y_{ij}^{obj} indicates if an object is present in a grid cell, and $\hat{p}_{ij}^{\text{obj}}$ is the predicted probability. The loss increases when the model is uncertain about true objects or falsely predicts objects where there are none, ultimately enhancing detection accuracy by refining object presence predictions. The mAP@50 (mean Average Precision at IoU threshold 0.5) measures the model's accuracy in object detection by averaging precision across all classes. In the mAP@50 equation, N represents the number of classes, and AP_i denotes the average precision for each class i, reflecting the accuracy of object detection at an IoU threshold of 0.5. It calculates how well predicted bounding boxes match the ground truth with at least 50% overlap. Our model reached an mAP@50 high value of 0.935 at 50 epochs.

References

(1) Park, H.-m.; Park, S.; de Guzman, M. K.; Baek, J. Y.; Cirkovic Velickovic, T.; Van Messem, A.; De Neve, W. MP-Net: Deep learning-based segmentation for fluorescence microscopy images of microplastics isolated from clams. *Plos one* **2022**, *17*, e0269449.

(2) Tkachenko, M.; Malyuk, M.; Holmanyuk, A.; Liubimov, N. Label Studio: Data labeling

software. 2020-2022; `https://github.com/heartexlabs/label-studio`, Open source software available from https://github.com/heartexlabs/label-studio.

(3) Perez, D.; Lie, T. T.; Weber, C. C. Relative electrode size and organic load effects on the energy storage efficiency of microbial electrolysis cells. *Bioresource Technology Reports* **2020**, *11*, 100518.

(4) Goh, C.-P.; Lim, P.-E. POTASSIUM PERMANGANATE AS OXIDANT IN THE COD TEST FOR SALINE WATER SAMPLES. *ASEAN Journal on Science and Technology for Development* **2017**, *25*, 383–393.